

On the application of the coupled finite-infinite element method to geodetic boundary-value problem

MICHAL ŠPRLÁK^{1,2}, ZUZANA FAŠKOVÁ³ AND KAROL MIKULA³

- 1 Research Institute of Geodesy and Cartography, Chlumeckého 4, 826 62 Bratislava, Slovakia (michal.sprlak@gmail.com)
- 2 Institute of Mathematical Sciences and Technology, Norwegian University of Environmental and Life Sciences, Drøbakveien 31, 1432, Ås, Norway
- 3 Department of Descriptive Geometry and Mathematics, Faculty of Civil Engineering, Slovak University of Technology, Radlinského 11, 813 68 Bratislava, Slovakia (faskova@math.sk, mikula@math.sk)

Received: July 13, 2010; Revised: February 22, 2011; Accepted: February 22, 2011

ABSTRACT

Our aim is to introduce the Coupled Finite-Infinite Element Method (CFIEM) as a new alternative approach to the Earth's gravity field modelling. We show that if the computational domain is large enough in radial direction, one can obtain the qualitatively and quantitatively comparable solution to the solution by the Finite Element Method (FEM). We study the influence of the size of the computational domain on the final CFIEM solution as well as the successive refinement of the discretization and its convergence to the exact solution. As an input data we use the synthetic boundary conditions computed from a Synthetic Earth Gravity Model (SEGM) and we test the CFIEM solution by the data generated directly from SEGM and the solution by the FEM.

Keywords: Coupled Finite-Infinite Element Method, Finite Element Method, Geodetic Boundary-Value Problem, Synthetic Earth Gravity Model

1. INTRODUCTION

Several groups of researchers have investigated the application of numerical methods for the solution of Geodetic Boundary-Value Problems (GBVPs) connecting the Laplace equation and Boundary Conditions (BCs) obtained by gravity measurements. Boundary element method solving boundary integral form of the GBVPs has been used in (Lehmann and Klees, 1999; Klees et al., 2001; Čunderlík et al., 2008; Čunderlík and Mikula, 2010). Variational method based on a weak form of GBVPs and minimization of quadratic functional has been preferred in (Holota, 1997; Holota and Nesvadba, 2008). Various GBVPs (e.g. linearized Molodensky, linearized fixed, altimetry-gravimetry) have been investigated in the previous studies where numerical solutions have been performed on a two-dimensional hypersurface represented by a sphere, ellipsoid or the Earth's surface.

In order to obtain numerical solution for the GBVPs in a three-dimensional domain, the Finite Element Method (FEM) on bounded domains has been applied. The pioneering work on two-dimensional domains has been done by *Meissl (1981)* and later, the GBVP with the Dirichlet and the Neumann (*Fašková, 2006; Fašková et al., 2007, 2010*) and the Dirichlet and the Newton (*Šprlák et al., 2006*) BCs have been introduced on three-dimensional domains. Using Coupled Finite-Infinite Element Method (CFIEM), the domain can be considered as unbounded and regularity condition is prescribed at infinity. Compared to the FEM, the advantage of this approach is that one obtains numerical solution in a three-dimensional domain with reduced amount of BCs.

In the present study, CFIEM is investigated and compared to FEM using a known solution for a unit sphere and a field generated by Synthetic Earth Gravity Model (SEGM). Formulation of the GBVP with the Dirichlet and the Neumann BCs is studied, CFIEM and FEM approaches are compared in the numerical experiments and results are emphasized in conclusions.

2. FORMULATION OF THE GBVP WITH MIXED BCs FOR CFIEM APPROACH

To define the GBVP with the Dirichlet and Neumann BCs we create the computational domain Ω infinite in radial direction and bounded by the limited part of the Earth's surface approximated by a sphere (Fig. 1a).

Let $T(\mathbf{x})$ be the disturbing potential satisfying the Laplace equation in Ω . Then the GBVP with the Dirichlet and the Neumann BCs for CFIEM is defined as follows:

$$-\nabla^2 T(\mathbf{x}) = 0, \quad \mathbf{x} \in \Omega, \quad (1)$$

$$\delta g(\mathbf{x}) = -\frac{\partial T(\mathbf{x})}{\partial r} \quad \text{on } \Gamma_{\text{Earth}}, \quad (2)$$

$$T(\mathbf{x}) = T^*(\mathbf{x}) \quad \text{on } \Gamma_{\text{Side Boundaries}}, \quad (3)$$

$$T(\mathbf{x}) \rightarrow 0, \quad \text{as } \mathbf{x} \rightarrow \infty. \quad (4)$$

For FEM approach we consider the radial boundary away from the Earth's surface Γ_{FE} :

$$-\nabla^2 T(\mathbf{x}) = 0, \quad \mathbf{x} \in \Omega_{FE}, \quad (5)$$

$$\delta g(\mathbf{x}) = -\frac{\partial T(\mathbf{x})}{\partial r} \quad \text{on } \Gamma_{\text{Earth}}, \quad (6)$$

$$T(\mathbf{x}) = T^*(\mathbf{x}) \quad \text{on } \Gamma_{\text{Side Boundaries}}, \quad (7)$$

$$T(\mathbf{x}) = T^*(\mathbf{x}) \quad \text{on } \Gamma_{FE}, \quad (8)$$

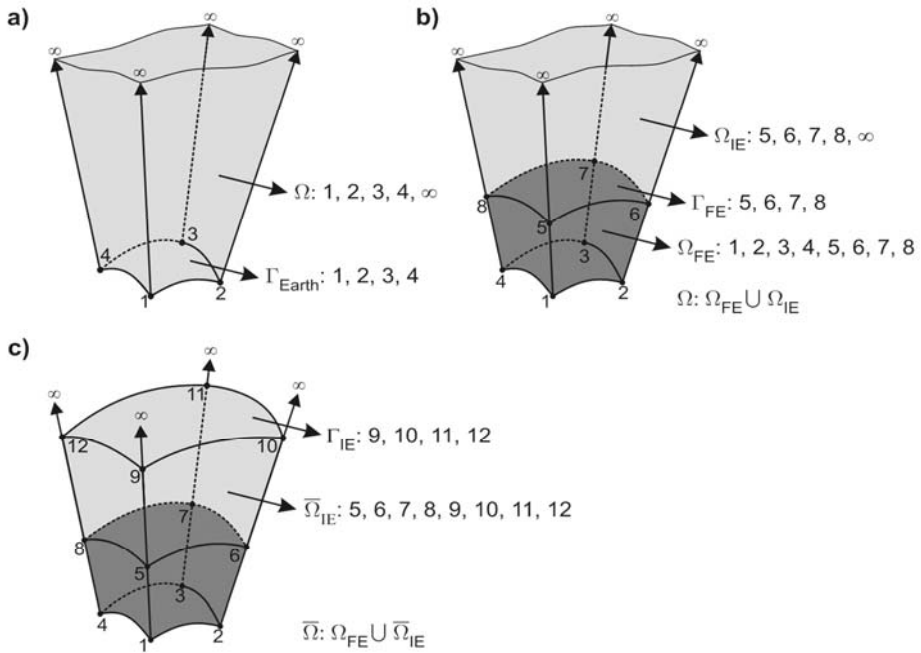


Fig. 1. a) Domain, b) decomposition of Ω into domains Ω_{FE} and Ω_{IE} , c) transformation of Ω into domain $\bar{\Omega}$.

where Ω_{FE} represents the finite domain depicted in Fig. 1b. Although the GBVP (Eqs.(1)–(4)) deals with an infinite domain, in Ansys (<http://www.ansys.com>) infinite-element method implementation we have to create an artificial boundary Γ_{IE} where the BC (Eq.(4)) is prescribed, see Fig. 1c, i.e., the finite domain $\bar{\Omega} = \Omega_{FE} \cup \bar{\Omega}_{IE}$ is created.

3. SOLUTION OF GBVP WITH THE MIXED BCs BY CFIEM

The idea of CFIEM has been originally published by *Marques and Owen (1984)* and *Zienkiewicz et al. (1985)*. Let's have the one-dimensional element which extends from node J with coordinate x_J through node K with coordinate x_K to the point M at infinity. This element is mapped onto the parent element defined by the local coordinate system in the range $-1 \leq \xi \leq 1$ using formula $x(\xi) = M_J(\xi)x_J + M_K(\xi)x_K$, where $M_J(\xi) = -2\xi/(1-\xi)$ and $M_K(\xi) = 1+2\xi/(1-\xi)$. It can be seen that $\xi = -1, 0, 1$ correspond to the global positions of $x = x_J, x_K, \infty$, respectively. Then let's consider a polynomial $P(\xi) = \alpha_0 + \alpha_1\xi + \alpha_2\xi^2 + \dots$ and if we substitute $\xi = 1 - 2(x_K - x_J)/r$ where r is the distance from the origin, we get $P(r) = \beta_0 + \beta_1/r + \beta_2/r^2 + \dots$. The

polynomial is required to decay to zero at infinity so $\beta_0 = 0$ and it is truncated at the quadratic r^{-2} term in the Ansys implementation. Then the finite element matrices are computed using Gauss quadratures applied on the transformed shape functions. In 2D or 3D, when only one direction is infinite, we proceed in the similar way as in 1D. More details about CFIEM approach can be found in (Bettess, 1992, Chap. 4) and in Ansys theory reference (<http://www.ansys.com>, Element Library: INFIN 110).

4. NUMERICAL EXPERIMENTS

All numerical computations have been performed using Ansys software. The first two experiments are theoretical to study the convergence of the solution to the exact one. We suppose a potential $u(r, \varphi, \lambda)$ generated by a unit sphere. In Experiment 1, we study the influence of the radial size of the computational domain to the final CFIEM solution. The domains, bounded by $\varphi \in \langle 0^\circ, 20^\circ \rangle$, $\lambda \in \langle 0^\circ, 20^\circ \rangle$ and various radii, have been meshed by the same size of elements. Results of FEM and CFIEM solutions are compared to the exact solution. The standard deviations of differences between numerical solutions u_{num}

and the exact solution u_{exact} , $\sigma_{num} = \sqrt{\sum_{i=1}^N (u_{exact_i} - u_{num_i})^2 / N}$, where N is number of nodes and $num = \text{FEM}$, resp. $num = \text{CFIEM}$, are presented in Table 1. It is evident that the CFIEM approach is very sensitive to the height of the domain and that the standard deviation decreases with an increase of the height of the domain. One can see that on the smallest domain the standard deviation of CFIEM approach is much higher than standard deviation of FEM approach with exact Dirichlet BC given on Γ_{FE} . On the other hand, standard deviations of FEM and CFIEM approaches are comparable on the largest domain.

In the Experiment 2, we have chosen the computational domain Ω_{FE} bounded by $\varphi \in \langle 0^\circ, 20^\circ \rangle$, $\lambda \in \langle 0^\circ, 20^\circ \rangle$, $r \in \langle 1.00 \text{ m}, 2.50 \text{ m} \rangle$ and $\bar{\Omega}_{IE}$ bounded by $\varphi \in \langle 0^\circ, 20^\circ \rangle$,

Table 1. Radial restrictions for the computational domains (2nd and 3rd column), number of nodes and standard deviations on the domain Ω_{FE} (4th, 5th and 6th column).

No.	Radial Restriction		Ω_{FE}		
	Ω_{FE} [m]	$\bar{\Omega}_{IE}$ [m]	$N_\varphi \times N_\lambda \times N_\Gamma$ No. of Nodes	σ_{FEM} [m ² s ⁻²]	σ_{CFIEM} [m ² s ⁻²]
1	(1.00, 1.50)	(1.50, 2.00)	11 × 11 × 11	0.000018	0.000207
2	(1.00, 1.75)	(1.75, 2.50)	11 × 11 × 16	0.000016	0.000053
3	(1.00, 2.00)	(2.00, 3.00)	11 × 11 × 21	0.000014	0.000021
4	(1.00, 2.25)	(2.25, 3.50)	11 × 11 × 26	0.000013	0.000014
5	(1.00, 2.50)	(2.50, 4.00)	11 × 11 × 31	0.000012	0.000012

$\lambda \in \langle 0^\circ, 20^\circ \rangle$, $r \in \langle 2.50 \text{ m}, 4.00 \text{ m} \rangle$. Afterwards, the domain Ω_{FE} has been meshed by $3 \times 3 \times 6$ elements and later three successive refinements have been performed. Our FEM and CFIEM solutions with linear elements have been compared to the exact solution. The standard deviations of differences between numerical solutions and the exact solution can be found in Table 2 and one can see that both methods give comparable results. The experimental Experimental Order of Convergence (EOC) for an error functional $E(h) > 0$, $EOC = (\log E(h_1) - \log E(h_2)) / (\log h_1 - \log h_2)$, where h is the maximal length of the edge of the element, can also be found in Table 2. The value of the EOC is equal to α if $E(h) \leq Ch^\alpha$, where $C > 0$ is a constant. The error functional $E(h)$ is given by the standard deviation of differences between the numerical and the exact solution.

In the Experiment 3, we have performed computations on the territory of Europe within the limits $\varphi \in \langle 36^\circ, 71^\circ \rangle$ and $\lambda \in \langle -11^\circ, 41^\circ \rangle$. Using the spherical harmonic coefficients of the SEGМ up to degree and order 360, BCs in the form of disturbing potential and gravity disturbances have been generated. We have created various computational domains by different radii and two sizes of the elements, 0.5° and 1.0° in spherical latitude and spherical longitude and approximately 55 km and 111 km in radial direction, have been applied. Due to simplicity, the Earth's surface Γ_{Earth} has been approximated by a reference sphere with radius $R = 6378$ km. Standard deviations of the differences on Γ_{Earth} between FEM and CFIEM solutions compared to SEGМ are shown in Table 3. When we compare the standard deviations on domains 1, 2 and 3 it is evident how big improvements can bring an extending of the computational domain. On the other hand, one can see that when the domain is large enough (domains 3, 4 and 5), the CFIEM gives comparable results to the FEM with prescribed exact Dirichlet values.

The differences between FEM and CFIEM solutions and SEGМ for the Dirichlet-Neumann BVP are depicted in Figs. 2 and 3.

Table 2. Number of nodes (1st column), standard deviations (2nd and 4th) and experimental orders of convergence (3rd and 5th) for the FEM and CFIEM approaches.

$N_\varphi \times N_\lambda \times N_\Gamma$ No. of Nodes (Ω_{FE})	$\sigma_{FEM}(\Omega_{FE})$ [m ² s ⁻²]	EOC_{FEM}	$\sigma_{CFIEM}(\Omega_{FE})$ [m ² s ⁻²]	EOC_{CFIEM}
$4 \times 4 \times 7$	0.00060178	---	0.00055739	---
$7 \times 7 \times 12$	0.00012338	2.28	0.00011812	2.23
$12 \times 12 \times 22$	0.00001897	2.45	0.00001894	2.34
$22 \times 22 \times 42$	0.00000557	2.07	0.00000686	1.77
$42 \times 42 \times 82$	0.00000125	2.15	0.00000265	1.37

Table 3. Radial restrictions for the computational domains (3rd and 4th column) and standard deviations on Γ_{Earth} between the CFIEM and FEM solutions and SEGM for the Dirichlet-Neumann GBVP (5th and 6th column).

No.	$\Delta\varphi \times \Delta\lambda$	Rad. Restr. (Ω_{FE}) [km]	Rad. Restr. ($\bar{\Omega}_{IE}$) [km]	σ_{FEM} [m ² s ⁻²]	σ_{CFIEM} [m ² s ⁻²]
1	1.0° × 1.0°	(6378, 7628)	(7628, 8878)	4.100	57.576
	0.5° × 0.5°	(6378, 7628)	(7628, 8878)	1.306	25.140
2	1.0° × 1.0°	(6378, 8878)	(8878, 11378)	4.096	6.461
	0.5° × 0.5°	(6378, 8878)	(8878, 11378)	1.328	5.269
3	1.0° × 1.0°	(6378, 11378)	(11378, 16378)	4.102	4.139
	0.5° × 0.5°	(6378, 11378)	(11378, 16378)	1.329	1.469
4	1.0° × 1.0°	(6378, 12628)	(12628, 18878)	4.098	4.108
	0.5° × 0.5°	(6378, 12628)	(12628, 18878)	1.325	1.364
5	1.0° × 1.0°	(6378, 13878)	(13878, 21378)	4.100	4.103
	0.5° × 0.5°	(6378, 13878)	(13878, 21378)	1.327	1.340

5. CONCLUSIONS

In this study a new approach to the Earth's gravity field modelling by using the CFIEM has been introduced. The GBVP with the Dirichlet and the Neumann BCs has been formulated for the proper application of the FEM and CFIEM approaches. The CFIEM solution has been compared to FEM solution with the exact Dirichlet BC given on upper boundary away from the Earth's surface, using a known solution for a unit sphere and a field generated by SEGM. In comparison to FEM, the main advantage of CFIEM approach is no necessity of BCs on upper boundary away from the Earth's surface. According to obtained results, we may conclude that although the CFIEM is very sensitive to the radial size of the domain, when the domain is large enough, the method is approximately second order accurate. More improvements of the numerical results for both, FEM and CFIEM approaches, can be achieved by finer discretization of the domain and by higher order basis functions.

Acknowledgments: Authors would like to thank to the Resort of Geodesy and Cartography in Slovakia for the financial support provided to Michal Šprlák to participate at the EGU 2010 and to APVV-0351-07 and VEGA 1/0269/09 grants.

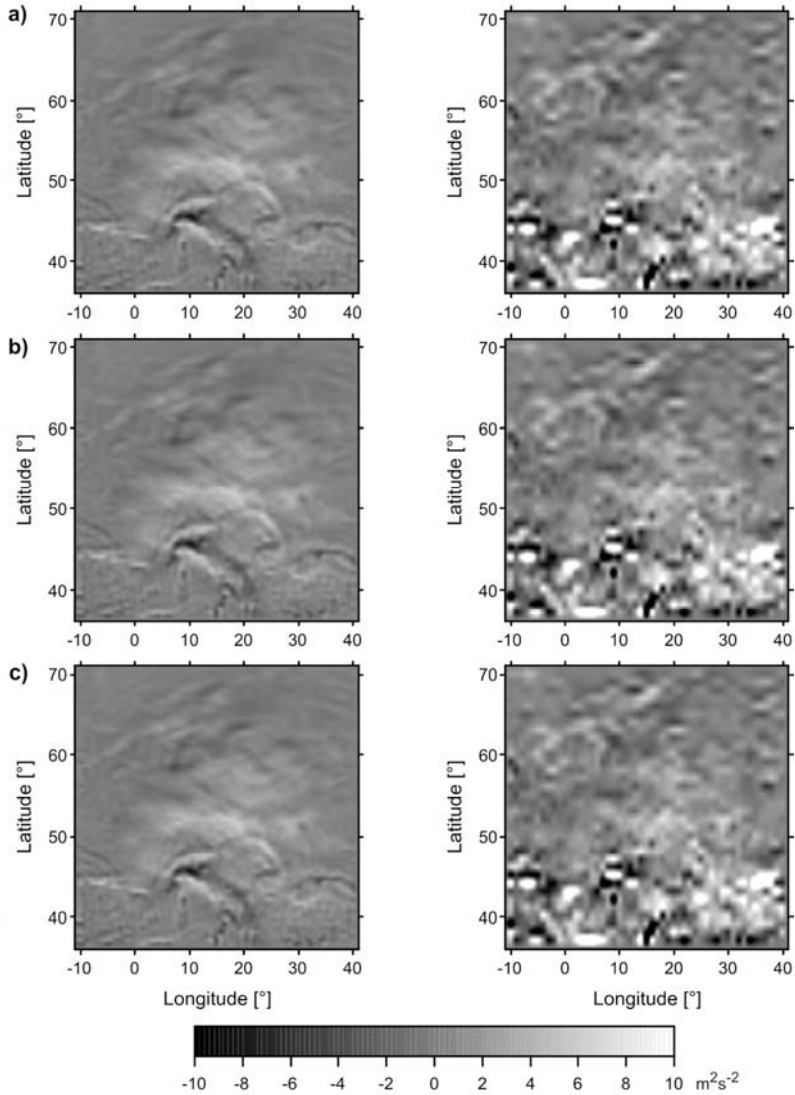


Fig. 2. Differences between the numerical solution obtained by the FEM and SEGM, discretization: (left) $0.5^\circ \times 0.5^\circ$, (right) $1.0^\circ \times 1.0^\circ$, radial restrictions of Ω_{FE} (km): **a)** (6378, 7628), **b)** (6378, 11378), **c)** (6378, 13878).

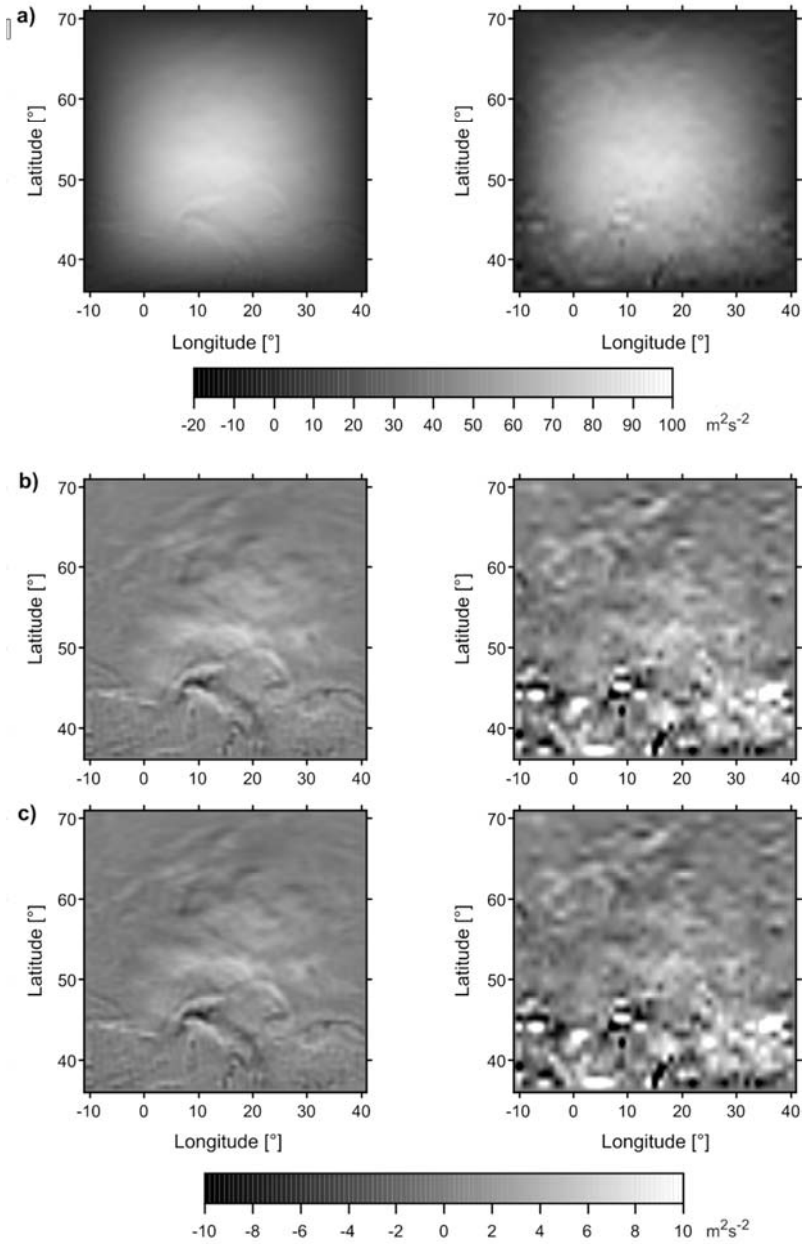


Fig. 3. Differences between the numerical solution obtained by the CFIEM and SEGM, discretization: (left) $0.5^\circ \times 0.5^\circ$, (right) $1.0^\circ \times 1.0^\circ$, radial restrictions of $\bar{\Omega}_{IE}$ (km): **a)** (7628, 8878), **b)** (11378, 16378), **c)** (13878, 21378).

References

- Bettess P., 1992. *Infinite Elements*. Penshaw Press, Sunderland, U.K. (http://www.bettess.co.uk/pete_web/pete_prof/books/ie1992/ie1992main.htm).
- Čunderlík R., Mikula K. and Mojžeš M., 2008. Numerical solution of the linearized fixed gravimetric boundary-value problem. *J. Geodesy*, **82**, 15–29.
- Čunderlík R. and Mikula K., 2010. Direct BEM for high-resolution global gravity field modelling. *Stud. Geophys. Geod.*, **54**, 219–238.
- Fašková Z., 2006. Application of the finite element method to the geodetic boundary value problem in Europe. *J. Electr. Eng.*, **57**, Special Issue, 39–42.
- Fašková Z., Čunderlík R., Janák J., Mikula K. and Šprlák M., 2007. Gravimetric quasigeoid in Slovakia by the finite element method. *Kybernetika*, **43**, 789–796.
- Fašková Z., Čunderlík R. and Mikula K., 2010. Finite element method for solving geodetic boundary value problems. *J. Geodesy*, **84**, 135–144.
- Holota P., 1997. Coerciveness of the linear gravimetric boundary-value problem and a geometrical interpretation. *J. Geodesy*, **71**, 640–651.
- Holota P. and Nesvadba O., 2008. Model refinements and numerical solution of weakly formulated boundary-value problems in physical geodesy. In: Xu P., Liu J. and Dermanis A. (Eds.), *VI Hotine-Marussi Symposium on Theoretical and Computational Geodesy*, International Association of Geodesy Symposia, **132**. Springer-Verlag, Heidelberg, Germany, 320–326.
- Klees R., van Gelderen M., Lage C. and Schwab C., 2001. Fast numerical solution of the linearized Molodensky problem. *J. Geodesy*, **75**, 349–362.
- Lehmann R. and Klees R., 1999. Numerical solution of geodetic boundary-value problems using a global reference field. *J. Geodesy*, **73**, 543–554.
- Marques J.M.M.C. and Owen D.R.J., 1984. Infinite elements in quasi-static materially non-linear problems. *Comput. Struct.*, **18**, 739–751.
- Meissl P., 1981. *The Use of Finite Elements in Physical Geodesy*. Report No. 313, Department of Geodetic Science and Surveying, The Ohio State University, Columbus, OH.
- Šprlák M., Fašková Z. and Mikula K., 2006. Application of the finite element method to the mixed geodetic boundary-value problem with Newton and Dirichlet boundary conditions. In: *MAGIA 2006: Mathematics, Geometry and Their Applications*. Slovak University of Technology, Bratislava, Slovakia, ISBN 80-227-2583-8, 23–32.
- Zienkiewicz O.C., Bando K., Bettess P., Emson C. and Chiam T.C., 1985. Mapped infinite elements for exterior wave problems. *Int. J. Numer. Methods Eng.*, **21**, 1229–1251.